Aerodynamic Wing Design for NAL's SST Using Iterative Inverse Approach

Kisa Matsushima
Fujitsu Ltd.
kisam@nal.go.jp

Toshiyuki Iwamiya
National Aerospace Laboratory
iwamiya@nal.go.jp

Sinkyu Jeong
Tohoku University
jeong@ad.mech.tohoku.ac.jp

Shigeru Obayashi
Tohoku University
obayashi@ad.mech.tohoku.ac.jp

Key Words: Design, SST, Wing

Abstract

Aerodynamic shape of a wing for NAL's SST has been designed by a supersonic inverse design method. This method handles SST's wing-fuselage configurations and provides wing section's geometry at every span. The design system consists of a new inverse problem solver and a Navier-Stokes simulation. The design procedure is iterative; the baseline shape is successively modified as the process of the inverse problem solver and Navier-Stokes simulation is iterated until the pressure distribution given by the designed wing can be regarded to converge to the target one. The design target is a NLF (natural laminar flow) wing for the wing-fuselage combination at the speed of $M_\infty = 2.0$. Several design constraints have been intended to be satisfied. By means of the method, a better wing shape which has much more desirable characteristics has been designed than that by the traditional linear theory.

1. Introduction

A next generation supersonic transport (SST) is of great interest in Japan as well as in Europe and the U.S. because of the projected trends of the world aviation market in the near future. Japan started an SST program in 1995 and will conduct the first flight test of National Aerospace Laboratory's experimental scaled SST in 2000. The program requires advanced CFD technology, especially to determine its aerodynamic shape[1]. The most effort needs to be put into developing design methods for determining the most aerodynamically efficient wing shape. This is because one of the most important challenges in designing a new SST is the improvement of the L/D ratio during cruising ($M_\infty = 2.0$).

We have been developing and verifying a numerical inverse design method for supersonic wings[2]. It is used to design the wing section geometry for a wing whose planform is fixed. Usually, the wing section design is performed in two steps; first, the warp curvature is determined three-dimensionally, then the thickness is prescribed two-dimensionally for each span section. Unlike most existing methods, our method treats both the warp curvature and the thickness distribution simultaneously, considering three-dimensional effects. The new method is based on the supersonic small disturbance equation and thin wing theory. The equations to solve the supersonic inverse problem are derived to be the integral equations shown in section 2. In section 3, the structure of the design system is described. In section 4, the new method is applied to a highly practical problem involving NAL's SST, in which the aim is to design a natural laminar flow wing for the wing-fuselage configuration. We also intend to satisfy design constraints such as the range of t/c_{max} of each span, and so on. The principals of the new method and the design results are presented.

2. Inverse problem for design

The basic idea of the inverse problem for the present design method is to define a mathematical function to relate pressure difference on a surface ΔCp to geometrical correction Δf. It should be emphasized that the formulation is finely done in Δ-form. Δf and ΔCp, variations from one state to another state of a flowfield, are used so that the method can gain wide applicability.

The formulation starts with the small disturbance approximation and thin wing theory. A wing is located at $z = 0$ in a supersonic flowfield whose free stream Mach number is M_∞. The x axis is streamwise, the y axis is spanwise, and the z axis is in the thickness direction of a wing.

The free stream velocity vector is assumed as $(1, 0, 0)$. A flow field is approximated by the linearlized small disturbance equation:

$$(1 - M_\infty^2)\overline{\phi}_{\overline{xx}} + \overline{\phi}_{\overline{yy}} + \overline{\phi}_{\overline{zz}} = 0 \qquad (1)$$

ϕ is a perturbation velocity potential. The shape of a wing is expressed as $f_{\pm}(\overline{x},\overline{y})$. + indicates the upper surface and − does the lower surface.

On the wing surface, the flow ought to be tangential to the surface as

$$\overline{\phi}_z(\overline{x},\overline{y},\pm 0)=\frac{\partial}{\partial \overline{x}}f_{\pm}(\overline{x},\overline{y}) \tag{2}$$

According to the linearized Bernoulli's theorem, the pressure coefficients on a wing surface are related to the perturbation velocity;

$$Cp_{\pm}(\overline{x},\overline{y})=-2\overline{\phi}_x(\overline{x},\overline{y},\pm 0) \tag{3}$$

+0 and -0 mean the upper and lower surface of a wing respectively.

Applying the Prandtl-Glauert transformation such as

$$x=\overline{x},\quad y=\beta\overline{y},\quad z=\beta\overline{z},\quad \phi(x,y,z)=\frac{1}{\beta^2}\overline{\phi}(\overline{x},\overline{y},\overline{z})$$

where $\beta=\sqrt{M_\infty^2-1}$

and taking variation of Eqs.(1-3) by changing ϕ to $\phi+\Delta\phi$, the equations for variation of the perturbation velocity potential, the correction in wing section shapes, and surface pressure difference between one state of the perturbation potential of ϕ and another one of $\phi+\Delta\phi$ are

$$-\Delta\phi_{xx}+\Delta\phi_{yy}+\Delta\phi_{zz}=0 \tag{4}$$

$$\frac{\partial}{\partial x}\Delta f_{\pm}(x,\frac{y}{\beta})=\beta^3\Delta\phi_z(x,y,\pm 0) \tag{5}$$

$$\Delta Cp_{\pm}(x,\frac{y}{\beta})=-2\beta^2\Delta\phi_x(x,y,\pm 0) \tag{6}$$

Now, we apply Green's theorem to Eq.(4) of a hyperbolic system and obtain $\Delta\phi$ in an analytical form,

$$\Delta\phi(x,y,z)=-\frac{1}{2\pi}\frac{\partial}{\partial x}\int\int_{\tau_+}\Big\{\big[\Delta\phi_\zeta(\xi,\eta,+0)-\Delta\phi_\zeta(\xi,\eta,-0)\big]\Psi(x,y,z;\xi,\eta,0)\Big\}d\xi d\eta$$
$$+\frac{1}{2\pi}\frac{\partial}{\partial x}\int\int_{\tau_+}\Big\{\big[\Delta\phi(\xi,\eta,+0)-\Delta\phi(\xi,\eta,-0)\big]\times\Psi_\zeta(x,y,z;\xi,\eta,0)\Big\}d\xi d\eta \tag{7}$$

where

$$\Psi(x,y,z;\xi,\eta,\zeta)=cosh^{-1}\frac{x-\xi}{\sqrt{(y-\eta)^2+(z-\zeta)^2}} \tag{8}$$

$$\Psi_\zeta(x,y,z;\xi,\eta,\zeta)=\frac{(x-\xi)(z-\zeta)}{[(y-\eta)^2+(z-\zeta)^2]}\times\frac{1}{\sqrt{(x-\xi)^2-(y-\eta)^2-(z-\zeta)^2}} \tag{9}$$

Then, the formulation is performed referring to Takanashi's method[3] which was developed for transonic wing ($M_\infty<1.0$) design. Unlike a transonic flowfield which is mainly an elliptic system, the influenced domain by the disturbance at $P(x,y,z)$ is limited. So the domain for integrations ,which is a portion of the physical space around a wing, should be carefully defined for Eq.(7). Since the influenced domain is behind the bow shock wave and inside the Mach forecone from $P(x,y,z)$, the integral domain is bounded with the two surfaces in the manner shown in the first figure of Fig.1. On the surface of the bow shock wave and the Mach cone, each integrand in Eq.(7) becomes zero. The surface integral domain where the integration remains nonzero is a portion of the wing surface which is bounded by the leading edge line and the hyperbola $(x-\xi)^2-(y-\eta)^2-(z)^2=0$. In Eq.(7), every integrand is divided into two functions, one is for the upper surface($\zeta=+0$) and the other is for the lower surface($\zeta=-0$). So, the domain τ_+ means the upper surface of the wing plane where $(x-\xi)^2-(y-\eta)^2-(z)^2\geq 0$. It is shown in Fig.1.

In order to expose the boundary condition ΔCp and the unknown shape function Δf as explicit functions, we do further calculus with Eq.(7). In fact, ΔCp is associated with $\Delta\phi_x$ and Δf is associated with $\Delta\phi_z$. Differentiating Eq.(7) with respect to x and adding $\Delta\phi_x(x,y,z)$ at $z=+0$ to $\Delta\phi_x(x,y,z)$ at $z=-0$ we obtain

$$\Delta w_s(x,y)=-\Delta u_s(x,y)-\frac{1}{\pi}\int\int_{\tau_+}\frac{(x-\xi)\Delta w_s(\xi,\eta)}{[(x-\xi)^2-(y-\eta)^2]^{3/2}}d\xi d\eta \tag{10}$$

where

$$\Delta u_s=\Delta\phi_x(x,y,+0)+\Delta\phi_x(x,y,-0)$$
$$=-\frac{1}{2\beta^2}(\Delta Cp(x,\frac{y}{\beta},+0)+\Delta Cp(x,\frac{y}{\beta},-0)) \tag{11}$$

$$\Delta w_s=\Delta\phi_z(x,y,+0)-\Delta\phi_z(x,y,-0)$$
$$=-\frac{1}{\beta^3}(\frac{\partial\Delta f(x,\frac{y}{\beta},+0)}{\partial x}-\frac{\partial\Delta f(x,\frac{y}{\beta},-0)}{\partial x}) \tag{12}$$

Similarly, differentiating Eq.(7) with respect to z and adding $\Delta\phi_z(x,y,z)$ at $z=+0$ to $\Delta\phi_z(x,y,z)$ at $z=-0$

$$\Delta w_a(x,y)=-\Delta u_a(x,y)+\frac{1}{\pi}\int\int_{\tau_+}\frac{(x-\xi)\Delta u_a(\xi,\eta)}{(y-\eta)^2\sqrt{(x-\xi)^2-(y-\eta)^2}}d\xi d\eta \tag{13}$$

where

$$\Delta u_a=\Delta\phi_x(x,y,+0)-\Delta\phi_x(x,y,-0)$$
$$=-\frac{1}{2\beta^2}(\Delta Cp(x,\frac{y}{\beta},+0)-\Delta Cp(x,\frac{y}{\beta},-0)) \tag{14}$$

$$\Delta w_a=\Delta\phi_z(x,y,+0)+\Delta\phi_z(x,y,-0)$$

$$= -\frac{1}{\beta^3}\left(\frac{\partial \Delta f(x, \frac{y}{\beta}, +0)}{\partial x} + \frac{\partial \Delta f(x, \frac{y}{\beta}, -0)}{\partial x}\right) \quad (15)$$

The same fundamental equations for pressure and surface geometry are found in Ref.[4].

Eq.(10) is a Volterra integral equation of the second kind for Δw_s, the thickness change at (x, y) on a wing, while Eq.(13) is the integral expression for Δw_a, the curvature change of the wing section camber, at (x, y). The geometrical correction is calculated using

$$\Delta f_{\pm}(x, \frac{y}{\beta}) = \frac{1}{2}\beta^3 \int_{L.E}^{x} \Big[\Delta W_s(\xi, y) \pm \Delta W_a(\xi, y)\Big] d\xi \quad (16)$$

Therefore, we can obtain the geometrical correction everywhere on a wing, specifying the difference between target and current pressures, $\Delta Cp = Cp^{target} - Cp^{current}$. There needs special treatment for the integration, because the integrands of Eqs.(10 and 13) become singular on the Mach cone. We calculate it using the limiting operation of improper integrals.

3. Design Procedure

The design procedure for supersonic wings is iterative method. Fig.2 describes the procedure. The method determines the wing section's geometry which realizes a specified target pressure distribution at all span stations of a wing. At the beginning, a baseline shape is to be guessed. Then the flow field around the wing is analyzed by flow simulation to get the current Cp distribution on the wing surface. Next the inverse problem is solved to obtain the geometrical correction value Δf corresponding to the difference between target and current pressure distributions ΔCp. The new wing is designed by modifying the baseline shape with Δf. Now, the current shape is updated. Then we go back to the analysis part, again. The flow analysis is conducted to see if the current shape realizes target pressure distribution. If the pressure difference between target and current ones is negligible, the design is completed. Otherwise, we proceed to solve the inverse problem and iterate the design loop until the pressure difference becomes negligible. This iterative procedure of reducing the residual is widely used for numerical aerodynamic design.

There are two primary parts; one is a flow analysis part which conducts grid generation and flow simulation. The other is a design part where the inverse problem is solved to update the wing geometry. Both part are completely independent from each other. So, any kind of simulation codes can be employed or even a wind tunnel testing can replace the analysis part as long as they provide the accurate pressure distribution on the wing surface. For the present project, a Navier-Stokes (N-S) simulation about a wing-fuselage configuration is conducted in the analysis part[5], so that the fuselage effect can be taken into for design. The designed geometry approximately includes the aerodynamical effect of interaction between the fuselage and the wing. This is for the sake of Δ-form formulation of the inverse problem.

4. Wing design for wing-fuselage combination

The wing of NAL's experimental scaled SST is aerodynamically designed at $M_\infty = 2.0$. The SST planform is illustrated in Fig. 3. To design high L/D wing, we prescribe a target pressure whose elliptical load distribution minimizes the induced drag and whose upper surface distribution can keep the laminar boundary layer as long as possible. We are going to design section geometry of the SST wing which realizes the Natural Laminar Flow on its upper surface and the optimum load distribution. For the computation, the half span of the wing is divided into 82 (spanwise) $\times$ 50 (chordwise) panels. The spanwise target load distribution, which is calculated from the prescribed target pressure on the upper and lower surfaces, is presented in Fig.4 by $\square$. The chordwise target pressure distribution at four span stations is shown in Figs.5-8 by chain lines, – - –.

As stated in the previous section, the design procedure of our method is iterative, and the wing design starts from the baseline model. The baseline shape of the wing is the result of the planform and warp optimizations in terms of the L/D ratio, while the shape of the fuselage is determined using area rule[1,6]. The thickness distribution of the NACA66003 airfoil is adopted as the chordwise thickness distribution for each span station of the wing. Despite those optimizations, the performance of the wing of the wing-fuselage model is not as efficient as expected. In Fig.4, for example, the spanwise load distribution of the baseline shape does not show good agreement with the target one. It is because those optimizations were done for a wing alone. In other words, they did not take the wing-fuselage interaction into consideration. Therefore, improvement on the aerodynamic shape of the SST wing by the method which can count the interaction effect is necessary. In addition, the method is useful for designing a NLF wing which has a typical profile of Cp distribution on the upper surface. The inverse problem solver we have developed gives geometry which realizes a specified Cp distribution. This is the advantage of the new method, in contrast with traditional methods which handle just a load, not Cp distribution itself.

Speaking of practical application, several modifications are introduced in the design loop. We make modification on the currently obtained wing geometry at every iteration step to satisfy design requirements which are constraints on the trailing edge and twisting axis. To guarantee that every section has a closed trailing edge, the solution ΔWs is modified such as

$$\Delta W_s^{mod}(x, y) = \Delta W_s(x, y) - \frac{\int_{L.E.}^{T.E.} \Delta W_s(\xi, y) d\xi}{\int_{L.E.}^{T.E.} d\xi} \quad (17)$$

so as to satisfy the condition:

$$\int_{L.E.}^{T.E.} \Delta W_s^{mod}(\xi, y) d\xi = 0 \qquad (18)$$

It is requested that the twisting axis of the wing of the SST goes through 70%-chord of every span section. Every point at 70%-chord on the mean line of a span section has to be on a straight line. However, the z location of the mean line of every span station moves at random after solving the inverse problem and it breaks the constraint on the twisting axis. Then, the geometry at every span station is let to move in the z direction so that every point at 70%-chord on the mean line can stay on a straight line. Theses modifications in ΔW_s and z location do not cause substantial difference in the realized pressure distribution from that by the geometry without modification.

Another modification is on the specified target pressure. In general, an arbitrarily specified pressure distribution dose not always correspond to a physically acceptable solution. Sometimes there might be no exact solution. Thus, the desired role of the inverse design method is to find the solution whose pressure distribution is closest to the specified target pressure. In this sense, the specified pressure distribution is not absolute. It should be modified if necessary in order to have the resulting geometry meet the design requirement. But the modification can be accepted as long as the modified target pressure would not disturb the upper surface NLF. In this project, we modify it to arrange the leading edge in an appropriate shape and to meet the thickness constraint. the third modification is made on the derived integral equations. In the vicinity of the wing tip the Eqs.(10) and (13) become invalid, because either the small disturbance approximation or thin wing theory does not hold the same order of accuracy as they do in the midway part of the wing. Thus, in the region of around the tip, we use the linearized two dimensional theory of supersonic airfoil such as

$$\Delta w_s(x, y) = -\Delta u_s(x, y) \qquad (19)$$

$$\Delta w_a(x, y) = -\Delta u_a(x, y) \qquad (20)$$

After a trial and error examination, the Eqs.(10) and (13) have been replaced with Eqs.(19) and (20) respectively in the region outer than 70%-span station of the wing.

The result is displayed in terms of the load in Fig.4. It shows the load by the designed wing along y-span compared with that of the target and the baseline. The realized load distribution can be considered almost optimum in terms of minimizing pressure drag. The design results at several span stations are shown in Figs.5-8. Fig.5 presents the wing section geometry and the realized pressure distribution along the chord at 30%-span station. The dashed line and '+' indicate the geometry and pressure distribution of the baseline wing section respectively, while the solid line and ◇ do those of the designed wing section. The target pressure is indicated by chain lines. Fig.6 shows the wing section geometry and pressure distribution at 50%-span station. Fig.7 shows those at 70%-span station. Fig.8 shows those at 90%-span station. The resulting wing realizes much closer pressure distribution to the target than the baseline wing dose. The one of the most important features of a NLF wing is the sudden expansion of the upper surface Cp distribution at the leading edge. Furthermore, on the upper surface, a flat roof type of Cp distribution along the chord is highly desirable to make turbulence transition take place as late as possible. These features can be seen in the target pressure distributions of Figs.5-8. At every span-station, the designed wing can materialize Cp distribution which has such good features of a NLF wing. In fact, the stability analysis has proven the improvement on the N-factor by the new method; the value of N has substantially reduced.

5. Conclusions

A three-dimensional supersonic inverse method has been developed and applied to the design of the wing of NAL's SST. The equations to solve the supersonic inverse problem were derived from the supersonic small disturbance equation and thin wing theory. They are the integral equations. Since the formulation for the inverse problem was done in Δ-form and analysis was conducted about a wing-fuselage configuration, this method could take the wing-fuselage interaction into consideration. Several modification techniques that did not violate the design concept were introduced to satisfy the design constraint and to make practical use of this method.

The currently designed wing by the new method has attained the desirable pressure distribution to reduce drag and realize a NFL wing. The results have certified that the method has the strong feasibility to achieve practical aerodynamic design of supersonic wings.

References

[1] Yoshida, K., Hayama, K.: "Numerical Methods for the Design and Analysis of Wings at Supersonic Speed," SAE Paper 91-2056. Oct., 1991.

[2] Jeong, S., Matsushima, K., Iwamiya, T. Obayashi, S., and Nakahashi, K.: "Inverse Design Method for Wings of Supersonic Transport," AIAA paper 98-0602, Jan., 1998.

[3] Takanashi, S.: "Iterative Three-dimensional Transonic Wing Design Using Integral Equations," J. Aircraft, Vol. 22, No. 8, pp. 655-660, Aug., 1985.

[4] Lomax, H., Heaslet, M. A. and Fuller, F. B.: "Integrals and Integral Equations in Linearized Wing Theory," NACA Rep. 1054, 1951.

[5] Takaki, R., Iwamiya, T., Aoki, A.: "CFD Analysis Applied to the Supersonic Research Airplain," 1st CFD Workshop on SST Design, March, 1998.

[6] Shinbo, Y., Yoshida, K., Iwamiya, T., Takaki, R., Mat-

sushima, K.: "Aerodynamic Design of Scaled Supersonic Experimental Airplane," 1st CFD Workshop on SST Design, March, 1998.

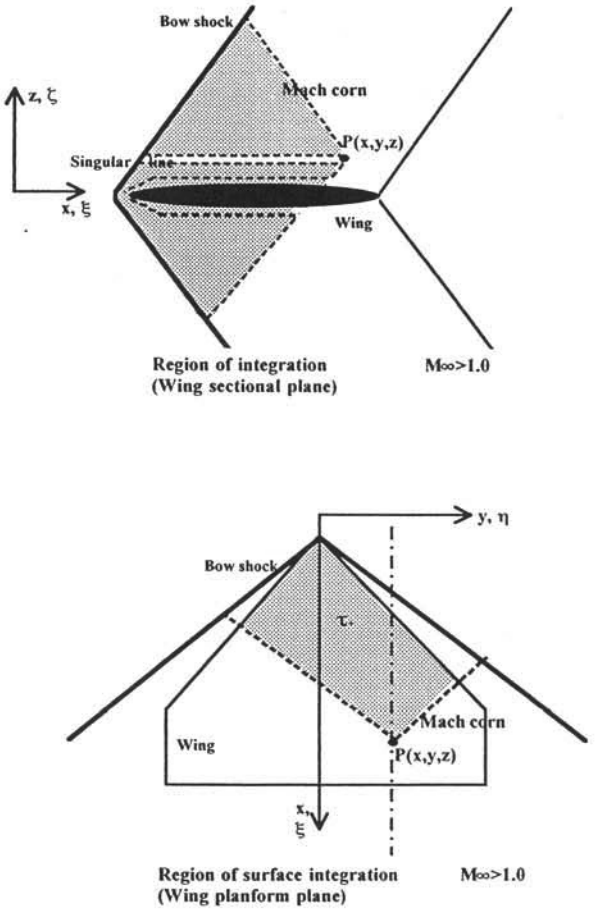

Fig. 1 Coordinate system for formulation.

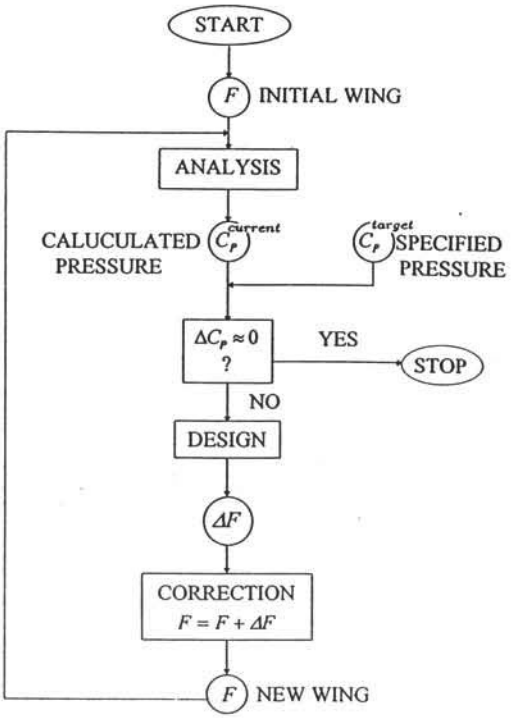

Fig. 2 Design procedure.

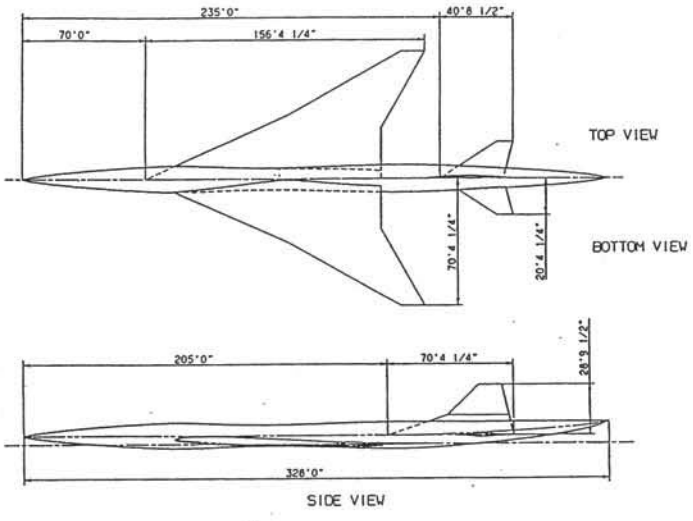

Fig. 3 SST planform.

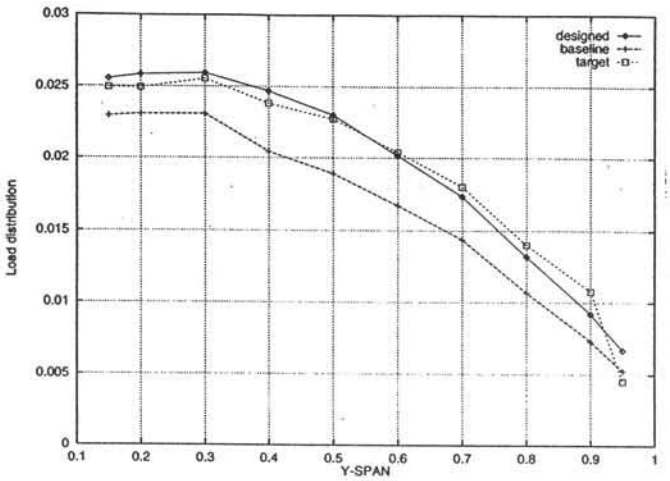

Fig. 4 Spanwise load distribution.
Load : + Baseline, □ Target, ◇ Designed

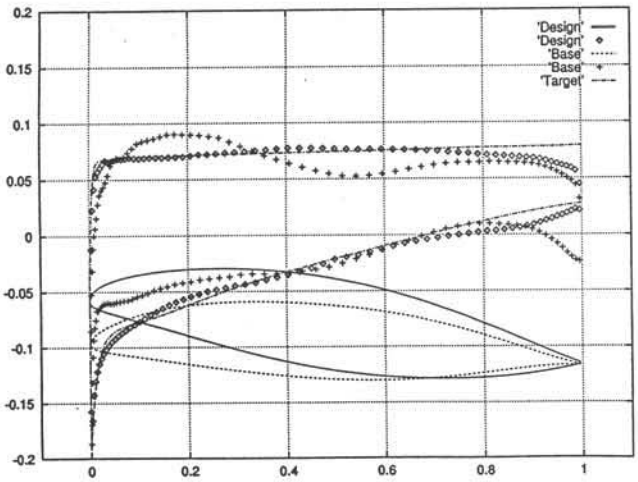

Fig. 5 Cp vs. chord at 30% span.
Pressure : + Baseline, −− Target, ◇ Designed
Wing Section : ··· Baseline, — Designed.

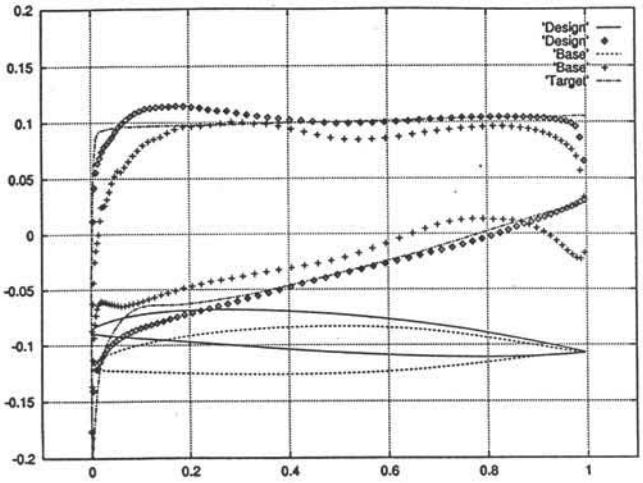

Fig. 6 Cp vs. chord at 50% span.

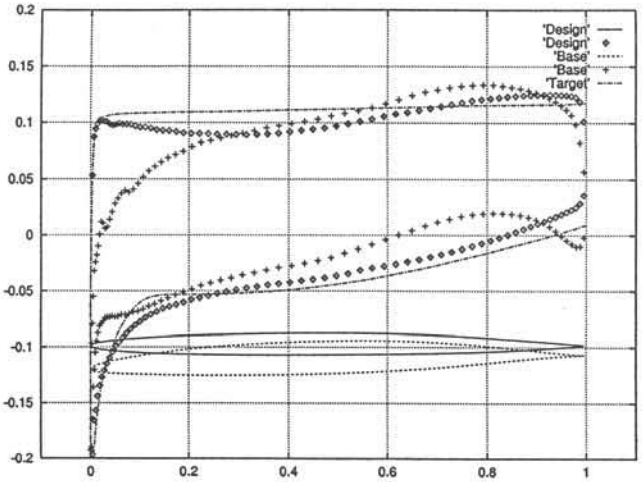

Fig. 7 Cp vs. chord at 70% span.

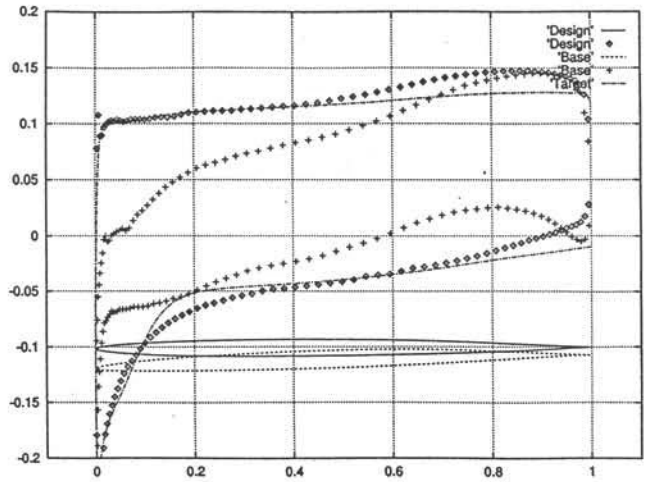

Fig. 8 Cp vs. chord at 90% span.